

# Conformation and Assembly of Polypeptide Scaffolds in Templating the Synthesis of Silica: An Example of a Polylysine Macromolecular “Switch”

Siddharth V. Patwardhan,<sup>\*,†,‡,§</sup> Ronak Maheshwari,<sup>‡</sup> Niloy Mukherjee,<sup>†</sup> Kristi L. Kiick,<sup>\*,‡</sup> and Stephen J. Clarson<sup>\*,†</sup>

Department of Chemical and Material Engineering, University of Cincinnati, Cincinnati, Ohio 45221-0012, Department of Materials Science and Engineering, University of Delaware, Newark, Delaware 19716, and Division of Chemistry, School of Biomedical and Natural Sciences, Nottingham Trent University, Nottingham, NG11 8NS, U.K.

Received September 27, 2005; Revised Manuscript Received November 16, 2005

Although the role of polycationic macromolecules in catalyzing the synthesis of silica structures is well established, detailed understanding of the mechanisms behind the production of silica structures of controlled morphologies remains unclear. In this study, we have used both poly-L-lysine (PLL) and/or poly-D-lysine (PDL) for silica synthesis to investigate mechanisms controlling inorganic morphologies. The formation of both spherical silica particles and hexagonal plates was observed. The formation of hexagonal plates was suggested, via circular dichroic spectroscopy (CD), to result from the assembly of helical polylysine molecules. We confirm that the formation of PLL helices is a prerequisite to the hexagonal silica synthesis. In addition, we present for the first time that the handedness of the helicity of the macromolecule does not affect the formation of hexagonal silica. We also show, by using two different silica precursors, that the precursor does not have a direct effect on the formation of hexagonal silica plates. Furthermore, when polylysine helices were converted to  $\beta$ -sheet structure, only silica particles were obtained, thus suggesting that the adoption of a helical conformation by PLL is required for the formation of hexagonally organized silica. These results demonstrate that the change in polylysine conformation can act as a “switch” in silica structure formation and suggest the potential for controlling morphologies and structures of inorganic materials via control of the conformation of soft macromolecular templates.

## Introduction

It is well-known that soft matter can be organized into various assemblies via molecular interactions such as van der Waals forces, hydrogen bonding, hydrophobic forces, and ionic interactions.<sup>1,2</sup> A wide range of molecules and macromolecules can participate in the formation of assembled structures, such as lipids and surfactants, polymers, peptides, and DNA,<sup>1–3</sup> and the assembled structures have well-documented application in areas such as biomedical materials, nanotechnologies, and scaffolds for inorganic materials.<sup>1–4</sup> Of particular interest in these investigations, soft matter has been used to synthesize inorganic materials of a variety of types and forms suitable for numerous applications;<sup>5–8</sup> for example, liquid crystal templates can be successfully employed for the generation of mesoporous molecular sieves.<sup>9–11</sup>

The technologically important silicon is found in large amounts in the Earth's crust (in the form of silicates) and in biological organisms (biosilica—as hydrated silica), where it is produced and deposited via environmentally benign conditions. The chemical production of silica, however, typically requires severe synthetic conditions such as extremes of pH, temperature, and/or the presence of solvents and may lead to the formation of problematic byproducts.<sup>12–14</sup> In addition, current chemically based synthetic procedures generally lack any morphological

control of the resulting silica. Biological organisms, in contrast, make use of biomolecules (e.g., peptides, proteins, and polysaccharides) and exhibit a remarkable ability to process soluble silicon compounds into organized and patterned hierarchical biosilica structures.<sup>15,16</sup> An increasing number of investigations have been conducted in order to understand the mechanisms involved in biosilicification, which might be useful in developing synthetic protocols for controlled silica synthesis. Organic molecules involved in biosilicification have been isolated from biosilicifying systems and characterized,<sup>16</sup> and the in vitro use of these bioextracts has shown that they precipitate particulate silica. However, these bioextracts fail to produce ornate structures resembling hierarchical biogenic silicas. In addition, the exact compositions and secondary conformations of these bioextracts remain unknown, and hence it is difficult to correlate the silica precipitation ability of these isolates with their structures. It has been postulated that proteins involved in calcite biomineralization control biomineral–protein interactions through protein secondary structural motifs and stereochemical preferences,<sup>5</sup> and the role of secondary structure in controlling porosity of silica structures has been demonstrated.<sup>17</sup> It has also been recently shown from in vitro studies that secondary conformation of peptides is indeed involved in controlling crystallization of calcite crystals.<sup>18,19</sup>

To understand biosilicification and to mimic the formation of biosilica, investigations have been undertaken using bioinspired analogues of bioextracts.<sup>20</sup> The formation of silica using assembled scaffolds/templates has also been demonstrated recently by several researchers (see ref 20 for details). Various

\* Corresponding authors. E-mail: Siddharth.Patwardhan@ntu.ac.uk (S.V.P.); Kiick@udel.edu (K.L.K.); Stephen.Clarson@uc.edu (S.J.C.).

<sup>†</sup> University of Cincinnati.

<sup>‡</sup> University of Delaware.

<sup>§</sup> Nottingham Trent University.

types of soft matter, such as peptides and polymers, have been employed in the formation of silica due to their functional properties<sup>21–26</sup> and their ability to form assembled structures.<sup>17,27–30</sup> However, only a few studies have succeeded in synthesizing novel silica structures utilizing bioinspired pathways. For example, Perry and Keeling-Tucker, using bioextracts isolated from plant biosilica, have synthesized crystalline silicas under ambient conditions, which would otherwise require harsh processing temperatures.<sup>31</sup> Cha et al., in investigations using tetraethoxysilane (TEOS) as the silica precursor, revealed that lysine–cysteine synthetic diblock copolypeptides were able to facilitate the formation of well-defined columnar silica structures in vitro.<sup>24</sup> The formation of fiber-like silicas via the use of either the synthetic polymer poly(allylamine hydrochloride) or the silaffin-derived R5-peptide<sup>32,33</sup> and the formation of sheetlike and hexagonal silica structures via the use of poly-L-lysine<sup>21,34,35</sup> have been reported by us and others. In this study, we present a detailed report on the successful synthesis of novel silica structures at neutral pH and under ambient conditions, using poly-L-lysine (PLL) and/or poly-D-lysine (PDL) as a polymer template. We demonstrate that the adoption of a helical conformation by polylysine of a given molecular weight is required for the formation of highly organized hexagonal silica plates and that a change in polylysine conformation can act as a “switch” in silica structure formation. Recently, Tomczak et al. published the combined poly-L-lysine molecular weight and conformation dependence in the formation of hexagonal silica from solutions of TMOS and PLL.<sup>35</sup> Although our work is complementary to their results, it is, however, distinct in the following aspects. We demonstrate that the shape of silica structures can be selected from hexagonal plates or particles via a change in the secondary conformation of PLL from  $\alpha$ -helix to  $\beta$ -sheet. In addition, we present for the first time that the handedness of the helicity of the macromolecule *does not* affect the formation of hexagonal silica. We also show, by using two different precursors, that the precursor *does not* have a direct effect on the formation of hexagonal silica plates. We confirm that the formation of PLL helices is a prerequisite to the hexagonal silica synthesis.

## Experimental Section

**Chemical Reagents.** Tetramethoxysilane (TMOS), 99+%, and water glass, which were used as the silica precursors, were purchased from Aldrich and Riedel-de Haën, respectively. Poly-L-lysine hydrochloride (PLL) (MW = 15 000–30 000) and poly-D-lysine hydrochloride (PDL) (MW = 15 000–30 000) were purchased from Sigma-Aldrich. The buffer used was 0.5 M potassium phosphate buffer at pH 7.0. Deionized ultrafiltered (DIUF) water was used for washing the centrifuged samples. Hydrochloric acid (HCl), used for the TMOS prehydrolysis, was obtained from Fisher. All reagents were used as received without any further purification.

**Silica Synthesis.** Silica synthesis was carried out as detailed elsewhere.<sup>36,37</sup> Two silica precursors, which have different chemistries, were used—tetramethoxysilane and sodium silicate. TMOS, an alkoxy silane, requires a catalyst to undergo hydrolysis and releases methanol upon hydrolysis and condensation. On the other hand, sodium silicate releases silicic acid and oligomers at pH 7 (i.e., in the buffer used herein). The latter has been claimed to mimic biological environments while the former is an attractive precursor for sol–gel synthesis. Detailed comparison of different precursors in bioinspired silica formation can be found elsewhere.<sup>38</sup> A stock solution of 1 mM HCl in DIUF water was prepared and was used for all the reactions. The TMOS solution in 1 mM HCl and the polymer solution in buffer were always freshly prepared for each experiment. A typical reaction mixture

contained 80  $\mu$ L of buffer, 20  $\mu$ L of peptide solution in buffer (of the desired concentration, 5 or 50 mg/mL), and 10  $\mu$ L of TMOS or water glass solution, and the [Si] was kept constant to ca. 100 mM. In the case where a mixture of PLL and PDL was used, 10  $\mu$ L (5 mg/mL solutions) of each peptide was added to the reaction medium. All the reactions were carried out at 20 °C, atmospheric pressure, and neutral pH. Upon the addition of peptides, the solutions were found to become cloudy within a few seconds and subsequent precipitation was observed. In control experiments, i.e., in the absence of any peptide, no precipitation was observed even after 24 h. After the desired reaction time, the samples were centrifuged at 14 000 rpm for 3 min. It was observed that a white solid precipitated in the tubes. The liquid was then removed, and DIUF water was added to the tubes. The precipitate was redispersed in the deionized water. This washing of samples was repeated three times to remove any free polypeptide. This dispersion was diluted further, and a few drops of this solution were placed on scanning electron microscope, transmission electron microscope, or atomic force microscope sample holders and were then left to dry under ambient conditions.

**Sample Characterization.** *Scanning Electron Microscopy (SEM) and Energy Dispersive Spectroscopy (EDS).* The dried samples were either coated with palladium and gold via evaporation or sputter coated with gold. They were then investigated using Hitachi S-4000, JEOL JSM-7400F, or JEOL JSM-840A scanning electron microscopes which were also equipped with EDS analysis capability.

*Atomic Force Microscopy.* The AFM measurements were performed under ambient conditions, using a Park Scientific Instruments (PSI) AutoProbe CP research scanning probe microscope. The measurements were in intermittent contact (IC), noncontact (NC), and contact modes to check for artifacts. Scan artifacts were also minimized by using multiple scans, different scan directions, and different size scans and sample rotations relative to the scan axes. The probes used were etched silicon ultralever probes from Thermomicroscopes with a nominal tip curvature of 10 nm. To maximize the lateral resolution, all images were taken in 512  $\times$  512 mode with an image size ( $<5 \times 5 \mu\text{m}^2$ ). Zeroth-order fit was used to flatten the images. Line profiles were formed by averaging several lines, which minimized noise.

*Transmission Electron Microscopy (TEM) and Selected Area Electron Diffraction (SAED).* Approximately 10–12 drops of the diluted silica solution was placed on a 3 mm carbon-coated grid in each case. The solution was then left to dry under ambient conditions overnight. Transmission electron microscopy was performed using either a Phillips CM20 or JEOL-2000FX 200kV TEM. Selected area electron diffraction (SAED) was used to check for crystallinity of the samples. Samples were tilted over a wide range of angles in an attempt to obtain a crystalline diffraction pattern.

*Circular Dichroism Analysis (CD).* Circular dichroic spectra were recorded on JASCO 810 spectrophotometer (Jasco, Inc., Easton, MD) in a 1 mm path length quartz cuvette in the single-cell mount setup. Background scans of buffer (0.1 M phosphate, pH 7) and hydrolyzed TMOS solution (0.05 M TMOS in 1 mM HCl) were recorded and manually subtracted from the sample scans. Polylysine solutions were made at a concentration of 0.6 mg/mL in 0.1 M phosphate buffer (pH 7) and mixed with hydrolyzed 0.1 M TMOS solution in a 9:1 ratio of polylysine/phosphate buffer to TMOS solution. The samples (200  $\mu$ L) were loaded into a 1 mm path length quartz cuvette to record the CD data. Data points for the wavelength-dependent CD spectra were recorded from 250 to 195 nm (at a speed 50 nm/min.) at every nanometer with a 1 nm bandwidth. CD data for spectrum 2 for the PDL system was collected from 250 to 198 nm because of excessively high absorbance at lower wavelengths that precluded the collection of accurate data below 198 nm. CD spectra are reported as intensity in millidegrees versus wavelength, owing to the uncertainty in the concentration of soluble polylysine during silicification.

*Infrared Spectroscopy.* All infrared spectroscopy measurements were conducted using a Magna IR-750 infrared spectrometer (Thermo Nicolet) fitted with a single-bounce diamond ATR (Grazebly Specac).

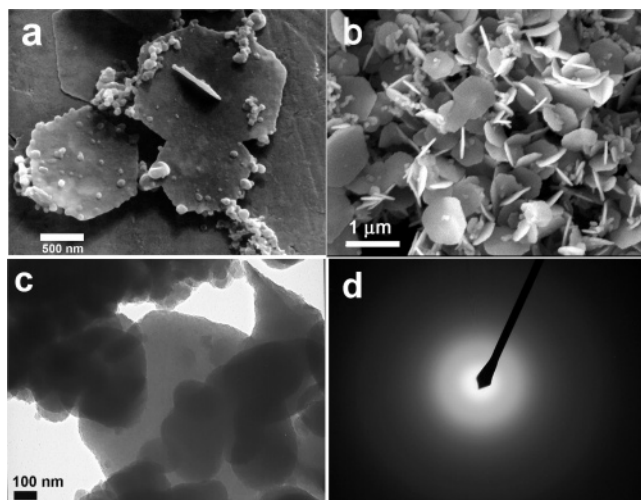


**Figure 1.** PLL-mediated formation of hexagonal silica under static conditions. SEM of hexagonal silica synthesized using (a) water glass and (b) TMOS. (c) TEM of hexagonal silica synthesized using TMOS and (d) corresponding SAED pattern of the hexagon shown in (c). Bars = (a) 500 nm, (b) 1  $\mu$ m, and (c) 100 nm.

The instrument was continuously purged with dry air for a minimum of 12 h prior to sample analysis. Spectrum collection parameters were set as follows: resolution set at 4  $\text{cm}^{-1}$ , interferometer speed 0.4747  $\text{cm s}^{-1}$ , averaging 512 scans.

**Thermogravimetric Analysis (TGA).** The TGA analysis was carried out using a TGA 2050 analyzer from TA instruments. The samples were heated from 30 to 900  $^{\circ}\text{C}$  at 10  $^{\circ}\text{C}/\text{min}$  under air.

## Results and Discussion

**Mechanisms Underpinning the Formation of Hexagonal Silicas.** TMOS and water glass were used as the silica precursors in experiments for PLL-mediated silica synthesis under quiescent conditions. Consistent with most reports of polypeptide-mediated silica synthesis,<sup>21,34,38,39</sup> these experimental conditions yielded a portion of the silica as spheres, as confirmed via transmission electron microscopy (TEM) and energy dispersive spectroscopy (EDS) of bulk samples. The selected area electron diffraction (SAED) pattern indicated the amorphous nature of these silica particles formed using PLL (see Figure S1 in the Supporting Information); these data are consistent with the X-ray diffraction results obtained from silica samples synthesized in the presence of another macromolecule in a related system.<sup>37</sup> However, in addition to particles, hexagons are also observed when either precursor is used, also consistent with previous reports by us and others.<sup>21,35,38</sup> The detailed mechanisms underpinning the formation of hexagonal silicas, however, are only recently being elucidated. Figure 1 shows a representative SEM of hexagonal particles that form under static conditions along with spherulike silica particles when water glass (Figure 1a) or TMOS (Figure 1b) was used as the silica precursor. It appears from parts a and b of Figure 1 that, although these precursors have different chemistries, the formation of spherical and hexagonal silica structures remains unaffected. Figure 1c presents typical TEM data from hexagonal and spherical silica samples precipitated using PLL and TMOS. One might have expected that these ordered hexagonal structures arise from atomic order (i.e., crystallinity); however, SAED analysis (Figure 1d) confirms the amorphous nature of the hexagons. Previous reports of the characterization of hexagonal silica plates via high-resolution cryo-TEM indicated crystallinity in the samples; however, the *d*-spacing observed matched those of PLL crystals,<sup>35</sup> thus

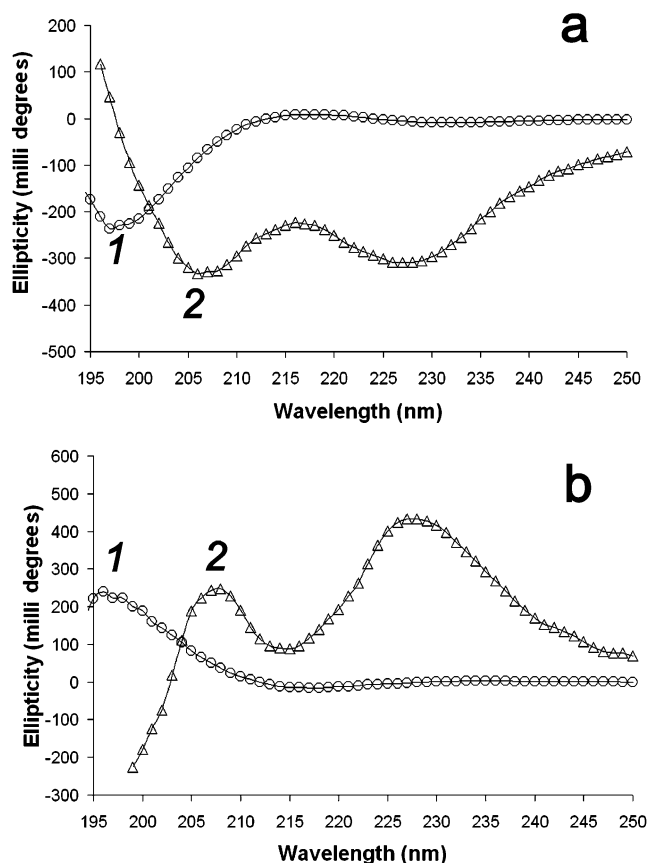
confirming that the silica in the hexagonal plates is amorphous in nature. Cui et al. have demonstrated that the water molecules associated with PLL molecules in hexagons (free from silica) are a part of PLL crystals, and hence dried samples fail to show any crystalline order.<sup>40</sup> These results may explain why we do not observe any crystallinity in the silica-PLL composite hexagons which were dried prior to analysis.

The formation of hexagonal structures likely results from the assembly of PLL into a hexagonal self-assembled structure. Indeed, Cui et al. have shown recently that poly-L-lysine is capable of forming hexagonal single crystals in aqueous solutions in the presence of anions.<sup>40</sup> Under the reported experimental conditions, the PLL molecules adopt a helical conformation in the presence of anions and subsequently pack into hexagonal single-crystal structures where water molecules are also a part of the single crystals. These helices were shown to be aligned perpendicular to the hexagonal plane; therefore the thickness of the single crystals was found to be dependent on the PLL molecular weight.<sup>40</sup> As polysilicic acids and silica particles are anionically charged at pH 7 (experimental conditions reported here), it is likely that the PLL folds and assembles via similar mechanisms, and due to its inherent ability to facilitate silicification, templates the formation of hexagonal silica structures as shown in Figure 1. Tomczak et al. have recently reported the combined molecular weight and conformation dependence in the formation of hexagonal silica from solutions of TMOS and PLL. In these previously reported studies, hexagonal silica structures were observed when the PLL employed in the silicification had a degree of polymerization (DP) of ca. 220, but not when the PLL had a DP of ca. 20,<sup>35</sup> and circular dichroic characterization confirmed the helical nature of only the longer PLL in the TMOS solution. Therefore, circular dichroic spectroscopy investigations were also employed here to determine the general viability of this hypothesis for the macromolecules of lower DP employed in these studies (PLL DP = 90–180); results of these analyses are shown in Figure 2.

As illustrated in Figure 2a, a solution of PLL in phosphate buffer (pH 7) yields a CD spectrum with a minimum at approximately 198 nm, indicative of a random coil conformation, as expected. Immediately upon addition of hydrolyzed TMOS solution, however, the solution yields a CD spectrum that approaches a maximum at wavelengths below 200 nm, with two minima at approximately 208 and 226 nm. These spectral features indicate an  $\alpha$ -helical conformation; the red-shift of the longer wavelength peak relative to the 222 nm minimum generally reported for the  $\alpha$ -helix is similar to that previously reported for aggregated  $\alpha$ -helices.<sup>41,42</sup> That these helical structures form in solutions of PLL and silica precursors (and not before addition of the silica precursors) corroborates the supposition that polylysine molecules of these intermediate molecular weights can form helices in the presence of negatively charged silica species and assemble into hexagonal arrays that mediate the formation of hexagonal silicas, which is also consistent with previous reports of the formation of silica plates from PLLs with DP between 100 and 840.<sup>21,35</sup>

Should simple hexagonal packing of helical macromolecules mediate the formation of hexagonal silica, such behavior should be equally likely for poly-D-lysine (PDL) as for PLL, as both could form helices, although of different chirality. As shown in Figure 2b, the CD spectra of PDL in phosphate buffer condition (either with or without hydrolyzed TMOS) show maxima and minima that mirror those of the PLL spectra, consistent with the different handedness of the PLL and PDL and

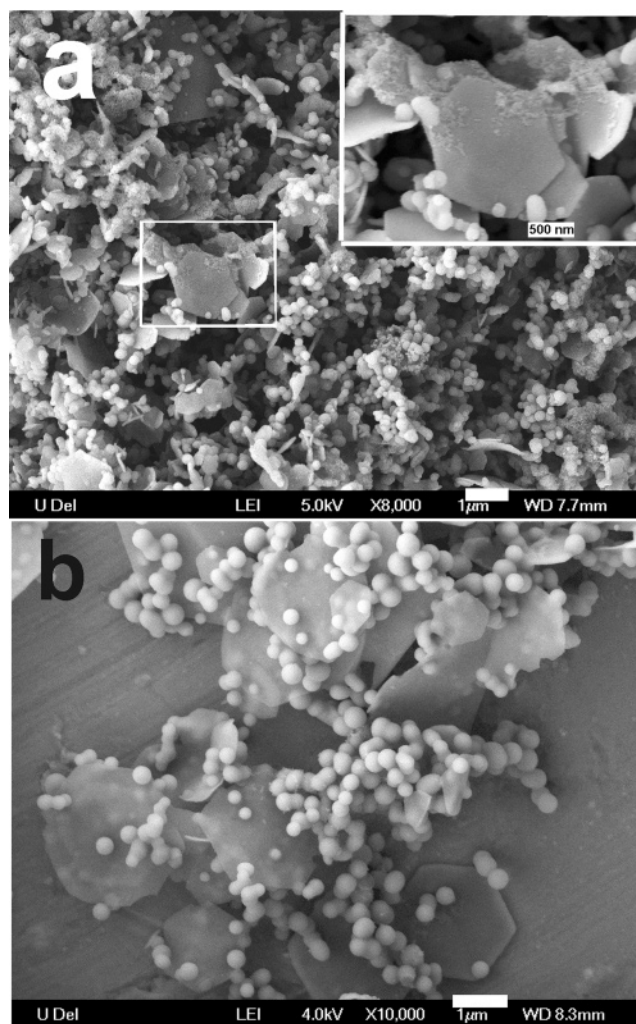




**Figure 2.** Circular dichroic spectra of (a) poly-L-lysine and (b) poly-D-lysine in phosphate buffer, pH 7 (curves 1) and in phosphate buffer, pH 7, with hydrolyzed TMOS solution (curves 2). CD spectra were collected at ambient temperature.

indicating that PDL also adopts an  $\alpha$ -helical conformation in the presence of silica precursors. The effect of PDL on silica synthesis was also probed; representative results are shown in Figure 3a. The data in Figure 3a clearly show the formation of hexagonal platelets (along with particles) from solutions of PDL and TMOS. When a mixture of PLL and PDL was added to the TMOS solution in buffer, similar silicas—spheres and hexagons—were precipitated as shown in Figure 3b, confirming that the adoption by polylysine of a helical conformation is a sufficient prerequisite for the formation of hexagonal silica platelets under these conditions.

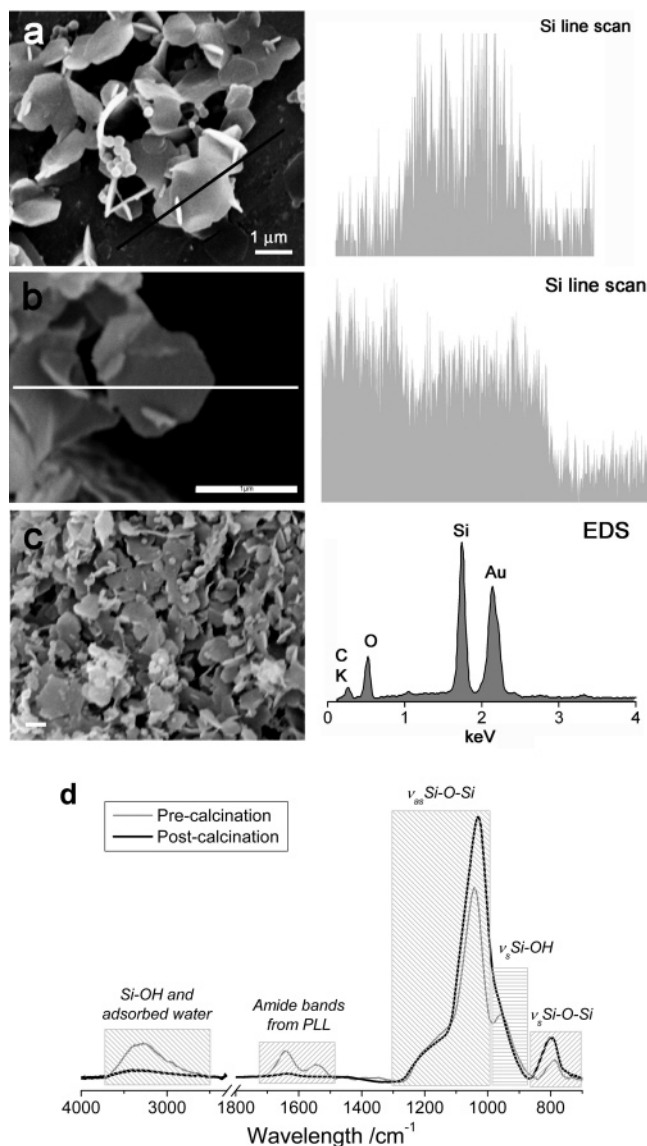
**Thermal Analysis of Silica–PLL Composites.** Elemental mapping confirmed that the hexagons were composed of silica (Figure 4a), which was also indirectly probed via thermal analysis, via calcination of the resulting samples at 600 °C for 1 h in order to remove occluded polylysine molecules. Representative SEM and EDS analysis performed on calcined samples showed that the hexagons retained their structure and silicate composition after removal of the organic phase (Figure 4b,c). The weight loss associated with the thermal treatment was nearly 16% (see Figure S2 in the Supporting Information). To further investigate the entrapment of polylysine molecules within silica, ATR-FTIR analysis of the samples before and after calcination was performed. Figure 4d shows overlaid spectra from 4000 to 700  $\text{cm}^{-1}$ . The predominant peak regions arising from polylysine and silica are highlighted on the plot and are as follows: 3700–2800  $\text{cm}^{-1}$  OH stretching modes from adsorbed water and silanol groups, 1720–1480  $\text{cm}^{-1}$  amide I and II bands from peptide, 1250–900  $\text{cm}^{-1}$  Si–O–Si asymmetric stretching and Si–OH symmetric stretching modes, and 800  $\text{cm}^{-1}$  Si–O–Si symmetric stretching modes. Upon calcination at 600 °C, the



**Figure 3.** PDL- and PLL + PDL-mediated formation of silica under static conditions. (a) Formation of hexagonal and spherical silica particles using PDL. The highlighted area is shown at higher magnification in the inset. (b) Hexagonal and spherical silica formed when a mixture of PLL and PDL was used. Bars = 1  $\mu\text{m}$  and 500 nm for the inset.

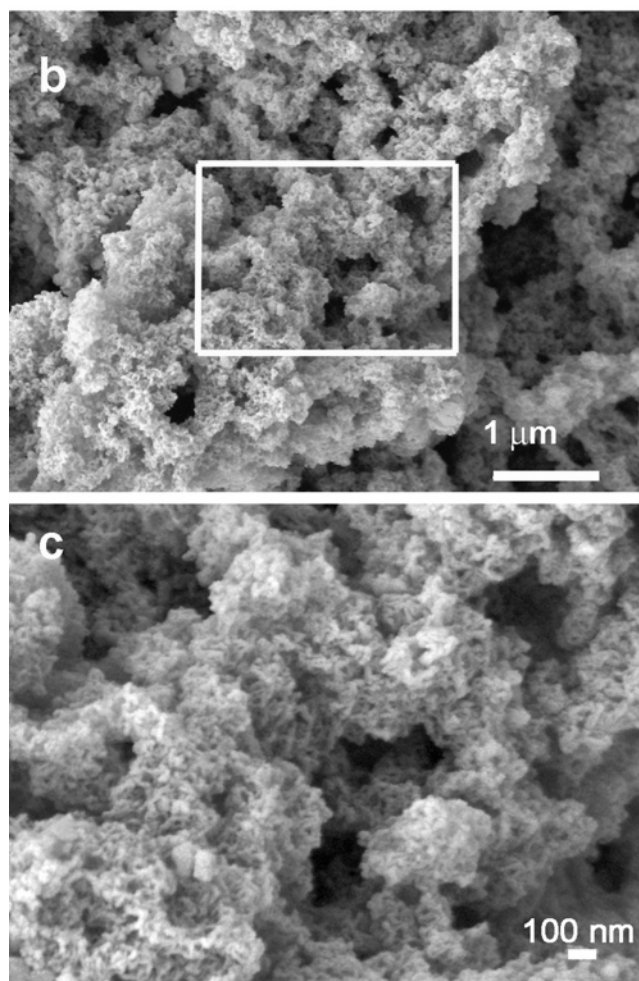
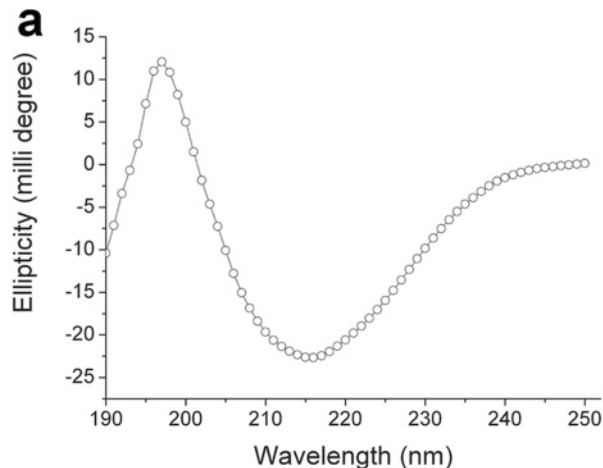
reduction in OH peaks and the disappearance of amide peaks is evident from Figure 4d, the latter confirming the loss of entrapped peptide. In addition, some variations in the silica peaks (1250–900  $\text{cm}^{-1}$ ) were also observed. As the peaks in this region are overlapped, deconvolution of these peaks into three components was performed: 1130–1115  $\text{cm}^{-1}$ , 1035–1045  $\text{cm}^{-1}$ , and 943–950  $\text{cm}^{-1}$  (see Figure S3 in the Supporting Information). The first two regions are assigned to longitudinal optical and transverse optical Si–O–Si asymmetric stretching peaks while the latter is assigned to Si–OH symmetric stretching modes.<sup>43</sup> Upon calcination, the silanol peak area reduced from 14% of the total peak area in the 1300–845  $\text{cm}^{-1}$  region to 7% which is due to the thermal condensation of silanol groups. The TGA and ATR-FTIR analysis provide the evidence for the presence of polylysine in silica samples, which degrades upon calcination thus confirming the templating effect of polylysine in silica formation. In addition, the combination of these CD, SEM, and EDS results clearly suggests that any polylysine helical species can mediate the formation of hexagonally organized silica structures, and more importantly corroborates the hypothesis that the formation of polylysine helices is a general mechanism in the formation of hexagonal silicas.

**PLL as a Macromolecular “Switch”.** To further confirm the role of polylysine helicity, apart from molecular weight



**Figure 4.** SEM, EDS, and ATR-FTIR analysis of hexagonal silica structures. SEM and EDS data before (a) and after calcination at 600 °C (b and c). (d) ATR-FTIR spectra of silica-PLL composites before and after thermal treatment.

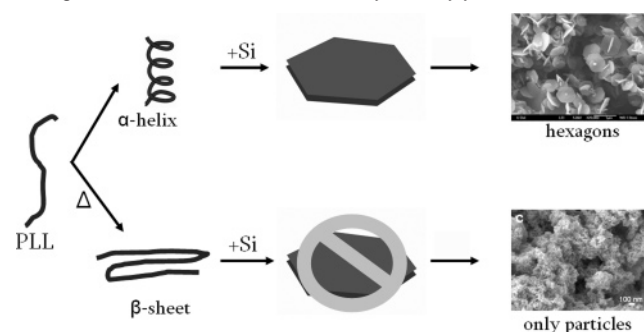
effects, in templating the formation of hexagonal silica, the PLL used in these investigations was converted to a  $\beta$ -sheet structure, via heating and subsequent cooling back to room temperature, prior to incubation with silica precursors. The PLL so treated was characterized via CD spectroscopy (Figure 5a); the presence in the CD spectrum of a maximum near 195 nm and a minimum near 218 nm confirmed the  $\beta$ -sheet conformation of the heat-treated PLL. The PLL was then added to an identical TMOS precursor solution as described above, and the resulting silica structures characterized via SEM. As shown in Figure 5, parts b and c, absolutely no hexagons—only particles—are observed, which clearly demonstrates the role of PLL secondary conformation in controlling silica morphology. Although the role of PLL molecular weight in silicification, as related to conformation, has been indicated by Tomczak et al.,<sup>35</sup> the data presented here unequivocally reveal that the adoption of a helical conformation by a PLL of a given molecular weight *is required* for the formation of hexagonally organized silica. Additionally, these results show that a change in polylysine conformation can act as a "switch" in silica structure formation. The role of PLL conformation in controlling the properties of other silica



**Figure 5.** (a) CD spectrum of PLL indicating  $\beta$ -sheet conformation, (b and c) SEM analysis of silica prepared using  $\beta$ -sheet PLL. The area highlighted in (b) is presented at higher magnification in (c). Bars = 1  $\mu$ m (b) and 100 nm (c).

structures has also been indicated in studies by Hawkins et. al, which have shown that the pore sizes of crystalline silica synthesized using PLL can be varied from <2 nm to 2–8 nm by changing the secondary conformation of PLL from  $\alpha$ -helix to  $\beta$ -sheet, respectively.<sup>17</sup> From the discussion above and the understanding gained about the mechanisms underpinning the formation of hexagonal silicas, a scheme is proposed for controlling silica formation from a PLL solution (Scheme 1). Polylysine molecules fold into  $\alpha$ -helices in the presence of silica



**Scheme 1.** Schematic Presentation of the Formation of Hexagonal Silica via the Self-Assembly of Polylysine Molecules<sup>a</sup>

<sup>a</sup> PLL molecules preassemble into helices and are packed into hexagons, which template hexagonal silica platelet formation. When PLL is converted to  $\beta$ -sheet conformation, no hexagonal silicas are formed, and networks of particles are precipitated instead.

precursors, which self-assemble into hexagonal structures, and then facilitate silicification. However, when PLL adopts a  $\beta$ -sheet conformation, no such assembly is possible, and only networks of silica particles are produced.

These results might also suggest that the complete organization of polylysine molecules into hexagonal assemblies would produce samples of solely hexagonal silicas, in contrast to the results shown above. Studies by Cui et al. and Tomczak et al. indicate that there is a minimum polylysine molecular weight (degree of polymerization; DP = 100) required to form helical structures in phosphate and TMOS solution, respectively.<sup>35,40</sup> Therefore, the breadth of the polylysine molecular weight in this study (DP ranging from ca. 90 to 180) likely results in the presence of some nonhelical PLL in solution, which subsequently results in nonhexagonal silicas. In addition, *all* polylysine molecules would have to be helical prior to the formation of any silica in order to promote exclusive formation of hexagonal plates, and it is likely that, regardless of the monodispersity of the polylysine, the competing kinetics of folding versus silicification may also cause the formation of spherical silica species. The formation of spherical assemblies using PLL has also been recently described by McKenna et al.<sup>30</sup> Taken together, the reported results demonstrate the potential for controlling morphologies and structure of inorganic materials strictly via control of the conformation of the soft macromolecular template. Furthermore, perturbation of the macromolecular template at the molecular level can alter the macroscopic properties of inorganic materials. Indeed, we have recently found that externally applied physical forces could be used to exploit this phenomenon, and the results obtained will be presented in due course. In addition, studies of silicification in the presence of lysine oligomers (monomer to pentamer) and PLL have revealed that lysine peptides play a significant role in catalyzing the early stages of silicic acid condensation and in promoting aggregation of particles, which is dependent on the peptide chain length, leading to the preparation of silicas with unique properties.<sup>25</sup> These observations suggest that polylysine fulfills multiple roles in silica formation—catalyst, template, and aggregation promoting agent.

### Conclusions

The investigations reported here demonstrate the role of poly-L-lysine and poly-D-lysine conformation in the formation of a range of novel silica structures under static conditions via a bioinspired route. Furthermore, they suggest the possibilities for selectively precipitating silica of controlled morphologies.

The perturbation of the PLL in the precursor solutions, via application of heat (conversion to  $\beta$ -sheet structure), results in the formation of different silica structures, likely as a result of hindrance to the formation of polylysine self-assembled structures. Accordingly, we have demonstrated that the adoption of a helical conformation by polylysine is *required* for the formation of hexagonally organized silica and that the change in polylysine conformation can act as a “switch” in silica structure formation. As we continue to investigate these and other related bioinspired systems, we hope to better understand and manipulate the role of (bio)macromolecules in silica synthesis *in vitro*.

**Acknowledgment.** It is a pleasure to thank DAGSI, European Union for funding our research as a part of the SILIBIOTEC project and the University of Delaware Research Foundation for the financial support of this research. We are grateful to Dr. C. Ni for his help in SEM and TEM analyses. We also thank Mr. Larry Grazulis and Ms. Kathy Gallardo for performing the AFM analysis and Mr. Paul Roach and Mr. David Belton for their help in performing ATR-FTIR and TGA analysis, respectively. We thank Dr. D. Pochan for sharing unpublished results. S.V.P. thanks Professor Carole C. Perry for various helpful discussions.

**Supporting Information Available.** Additional figures from the SEM, TEM, SAED, and AFM analysis of spherical silica particles formed using PLL, weight loss associated with the thermal treatment of silica–PLL composites, and deconvolution of ATR-FTIR spectra. This material is available free of charge via the Internet at <http://pubs.acs.org>.

### References and Notes

- (1) de Gennes, P. G. In *Nobel Lectures, Physics 1991–1995*; Ekspeng, G., Ed.; World Scientific Publishing Co.: Singapore, 1997.
- (2) Faul, C. F. J.; Antonietti, M. *Adv. Mater.* **2003**, *15*, 673.
- (3) Hamley, I. W. *Angew. Chem., Int. Ed.* **2003**, *42*, 1692.
- (4) Niemeyer, C. M. *Angew. Chem., Int. Ed.* **2001**, *40*, 4128.
- (5) Addadi, L.; Weiner, S. *Proc. Natl. Acad. Sci. U.S.A.* **1985**, *82*, 4110–4114.
- (6) Yu, S.-H.; Cölfen, H.; Antonietti, M. *J. Phys. Chem. B* **2003**, *107*, 7396–7405.
- (7) Slocik, J. M.; Wright, D. W. *Biomacromolecules* **2003**, *4*, 1135.
- (8) Sone, E. D.; Zubarev, E. R.; Stupp, S. I. *Angew. Chem., Int. Ed.* **2002**, *41*, 1706.
- (9) Kresge, C. T.; Leonowicz, M. E.; Roth, W. J.; Vartuli, J. C.; Beck, J. S. *Nature* **1992**, *359*, 710–712.
- (10) Beck, J. S.; Vartuli, J. C.; Roth, W. J.; Leonowicz, M. E.; Kresge, C. T.; Schmitt, K. D.; Chu, C. T. W.; Olson, D. H.; Sheppard, E. W.; McCullen, S. B.; Higgins, J. B.; Schlenker, J. L. *J. Am. Chem. Soc.* **1992**, *114*, 10834–10843.
- (11) Huo, Q.; Margolese, D. I.; Stucky, G. D. *Chem. Mater.* **1996**, *8*, 1147–1160.
- (12) Stober, W.; Fink, A.; Bohn, E. *J. Colloid Interface Sci.* **1968**, *26*, 62.
- (13) Iler, R. K. *The Chemistry of Silica*; John Wiley & Sons: New York, 1979.
- (14) Brinker, C. J.; Scherer, G. W. *Sol–Gel Science: The Physics and Chemistry of Sol–Gel Processing*; Academic Press: Boston, MA, 1990.
- (15) Simpson, T. L.; Volcani, B. E., Eds. *Silicon and Siliceous Structures in Biological Systems*; Springer-Verlag: New York, 1981.
- (16) Muller, W. E. G. *Silicon Biomineralization*; Springer: Berlin, 2003.
- (17) Hawkins, K. M.; Wang, S. S.-S.; Ford, D. M.; Shantz, D. F. *J. Am. Chem. Soc.* **2004**, *126*, 9112.
- (18) DeOliveira, D. B.; Laursen, R. A. *J. Am. Chem. Soc.* **1997**, *119*, 10627.
- (19) Kasparova, P.; Antonietti, M.; Cölfen, H. *Colloids Surf., A* **2004**, *250*, 153.
- (20) Patwardhan, S. V.; Clarson, S. J.; Perry, C. C. *Chem. Commun.* **2005**, *9*, 1113–1121.
- (21) Patwardhan, S. V.; Mukherjee, N.; Steinitz-Kannan, M.; Clarson, S. J. *Chem. Commun.* **2003**, *10*, 1122–1123.

- (22) Mizutani, T.; Nagase, H.; Fujiwara, N.; Ogoshi, H. *Bull. Chem. Soc. Jpn.* **1998**, *71*, 2017–2022.
- (23) Coradin, T.; Durupthy, O.; Livage, J. *Langmuir* **2002**, *18*, 2331–2336.
- (24) Cha, J. N.; Stucky, G. D.; Morse, D. E.; Deming, T. J. *Nature* **2000**, *403*, 289–292.
- (25) Belton, D.; Paine, G.; Patwardhan, S. V.; Perry, C. C. *J. Mater. Chem.* **2004**, *14*, 2231–2241.
- (26) Sudheendra, L.; Raju, A. R. *Mater. Res. Bull.* **2002**, *37*, 151.
- (27) Meegan, J. E.; Aggeli, A.; Boden, N.; Brydson, R.; Brown, A. P.; Carrick, L.; Brough, A. R.; Hussain, A.; Ansell, R. J. *Adv. Funct. Mater.* **2004**, *14*, 31–37.
- (28) Kroger, N.; Lorenz, S.; Brunner, E.; Sumper, M. *Science* **2002**, *298*, 584–586.
- (29) Knecht, M. R.; Wright, D. W. *Chem. Commun.* **2003**, 3038–3039.
- (30) McKenna, B. J.; Birkedal, H.; Bartl, M. H.; Deming, T. J.; Stucky, G. D. *Angew. Chem., Int. Ed.* **2004**, *43*, 5652–5655.
- (31) Perry, C. C.; Keeling-Tucker, T. *Chem. Commun.* **1998**, 2587–2588.
- (32) Patwardhan, S. V.; Mukherjee, N.; Clarson, S. J. *J. Inorg. Organomet. Polym.* **2001**, *11*, 117–121.
- (33) Naik, R. R.; Whitlock, P. W.; Rodriguez, F.; Brott, L. L.; Glawe, D. D.; Clarson, S. J.; Stone, M. O. *Chem. Commun.* **2003**, 238–239.
- (34) Rodriguez, F.; Glawe, D. D.; Naik, R. R.; Hallinan, K. P.; Stone, M. O. *Biomacromolecules* **2004**, *5*, 261–265.
- (35) Tomczak, M. M.; Lawrence, C.; Drummy, L. F.; Sowards, L. A.; Glawe, D. C.; Stone, M. O.; Perry, C. C.; Pochan, D. J.; Deming, T. J.; Naik, R. R. *J. Am. Chem. Soc.* **2005**, *127*, 12577.
- (36) Kroger, N.; Deutzmann, R.; Sumper, M. *Science* **1999**, *286*, 1129–1132.
- (37) Patwardhan, S. V.; Mukherjee, N.; Clarson, S. J. *Silicon Chem.* **2002**, *1*, 47.
- (38) Patwardhan, S. V.; Raab, C.; Husing, N.; Clarson, S. J. *Silicon Chem.* **2003**, *2*, 279.
- (39) Patwardhan, S. V.; Mukherjee, N.; Clarson, S. J. *J. Inorg. Organomet. Polym.* **2001**, *11*, 193–198.
- (40) Cui, H.; Krikorian, V.; Thompson, J.; Nowak, A. P.; Deming, T. J.; Pochan, D. J. *Macromolecules* **2005**, *38*, 7371.
- (41) Pandya, M. J.; Spooner, G. M.; Sunde, M.; Thorpe, J. R.; Rodger, A.; Woolfson, D. N. *Biochemistry* **2000**, *39*, 8728–8734.
- (42) Frost, D. W. H.; Yip, C. M.; Chakrabarty, A. *Biopolymers* **2005**, *80*, 26–33.
- (43) Fidalgo, A.; Ilharco, L. M. *J. Non-Cryst. Solids* **2001**, *283*, 144–154.

BM050717K